

Research report

Rhythmic and discrete elements in multi-joint coordination

Dagmar Sternad*, William J. Dean

Department of Kinesiology, The Pennsylvania State University, 266 Rec Hall, University Park, PA 16803, USA

Accepted 10 July 2003

Abstract

Everyday actions invariably consist of a combination of discrete and rhythmic elements within or across joints. The study investigated constraints arising from the co-occurrence of the two actions in a two-joint task and how endpoint trajectories are shaped due to these action elements at the joint level. The task consisted of an elbow oscillation in the plane that was to be merged with a fast discrete adduction or abduction in the shoulder triggered by an auditory signal. The task was performed with and without explicit instruction about the joint involvement. Two hypotheses were tested: (1) kinematic constraints for the coupling of discrete and rhythmic elements arise at the neuro-muscular level, such that EMG bursts of the discrete and rhythmic movement have a tendency to synchronize. This effect was documented previously in a comparable single-joint task. (2) The merging of the two elements is constrained by intersegmental torques such that initiation and performance of the discrete movement utilizes interaction torques. This hypothesis rests on the assumption that the CNS has an internal model of the limb dynamics and exploits passive torques. Key results support hypothesis 1: (i) the discrete action's initiation at the shoulder was constrained to a preferred phase of the ongoing elbow oscillation. (ii) The rhythmic elbow movement showed a systematic phase advance during the discrete shoulder shift, similar to those reported for the single-joint variant of the task. Reaction times of the discrete movement were longer and peak velocities slower than reported for isolated discrete movements, due to the simultaneous presence of the oscillation. (iii) Interaction torques acting from the elbow onto the shoulder joint were not selectively exploited for the acceleration of the discrete shoulder movement. Indirectly however, hypothesis 2 also found support: torques at the elbow generated compensatory muscle activity in the shoulder that stabilized the stationary joint. It was this rhythmic activity that posed the direct constraints on the initiation of the discrete movement.

© 2003 Elsevier B.V. All rights reserved.

Theme: Motor systems and sensorimotor integration

Topic: Control of posture and movement

Keywords: Rhythmic movement; Discrete movement; Multi-joint movement; Interaction torque; Reciprocal inhibition

1. Introduction

Almost all movements as they occur in daily life consist of cyclic and translatory components. Sometimes these rhythmic and discrete elements are concatenated into a movement sequence, other times they happen simultaneously and are performed by different effectors or different joints. An example for this interplay of rhythmic and discrete elements are gestures in the production of speech where the opening and closing of the lips occur in a quasi-rhythmic fashion but these actions are continuously

modulated with target-directed protrusion, retraction, or rounding of the lips or tongue to shape the air flow for different vowels and consonants. Another example is playing the piano which is frequently investigated in rhythmic tapping tasks as the archetypal rhythmic movement. However, the fully-fledged action consists not only of the precise timing of repeated key strokes by the fingers but also includes the goal-directed translatory action of the wrist and elbow joints that carry the hand across the keys. Rhythmic and discrete elements are distributed to different joints that are involved in the action. Similarly and lastly, the more mundane activity of cleaning a table provides an example where the usually cyclic wiping actions of the hand around the wrist or elbow joint are combined with a translation of the hand and arm across the table surface. It

*Corresponding author. Tel.: +1-814-863-7369; fax: +1-814-863-7360.

E-mail address: dxs48@psu.edu (D. Sternad).

is this task that will be investigated in a controlled form in the present study.

These examples raise awareness of the ubiquitous co-existence of rhythmic and discrete elements in functional everyday tasks and skills. Yet to date, research in motor control has commonly investigated either rhythmic or discrete movements. In focus is either the timing of rhythmic tapping, or the goal-directed control of a reaching movement, either rhythmic interlimb coordination, or accuracy in pointing. As a consequence of this separation, theoretical perspectives tend to diverge, depending on which class of movements is under study. Computational or cognitive accounts have tended to prevail in the literature on discrete movements such as pointing or reaching [38,39,43,49,61]. On the other hand, studies within the dynamical systems framework have focused almost exclusively on rhythmic movements, ranging from bimanual and locomotory coordination to polyrhythmic actions [2,4,29,55]. What is needed is to go beyond these isolated classes of actions and study more complex tasks and thereby cut across the theoretical perspectives.

Several previous studies already examined tasks consisting of rhythmic and discrete action elements in single-joint and bimanual actions [1,7,14,44,54,56,57,59]. In our own work, we proposed that the complex trajectories observed at the endpoint of the effector can be understood as the result of a merging of the two ‘movement primitives’, rhythmic and discrete patterns. This hypothesis was partially motivated by the fact that in nonlinear dynamical systems two major attractor types exist, fixed point and limit cycle attractors. We proposed that these two basic stable regimes are regarded as the major units of action for discrete and rhythmic movements, respectively [56,57]. If two stable regimes are fundamental in shaping the movement output, the question is how do they co-exist or interact.

With this objective we examined a single-joint elbow rotation task that involved an ongoing oscillatory action that was combined with a discrete translation of the elbow elicited by a randomly timed signal [7,56–59]. We showed that, due to the task-enforced co-existence of both elements, constraints arise that shape the performance. Results showed that the initiation of the discrete movement was indeed constrained to a limited phase window of the ongoing rhythmic movement, although the task required initiation at all phases. Peak velocity of the discrete movement was dependent on the frequency of oscillation. The ongoing oscillation was briefly perturbed but resumed its stable amplitude and period immediately after the discrete movement, i.e. the phase of the oscillation was reset. We proposed that these features reflect fundamental constraints in the central nervous system when combining goal-directed discrete movements with rhythmic movements. We replicated these findings in a simple model, inspired by the half-center model for neural oscillations, which consisted of two units mutually inhibiting each other

[34,35]. Depending on the type of activation signal, the pattern generator produced either a rhythmic or a discrete output when driving a mechanical limb. If the two control signals were coupled by summation, the activation of the neural system produced discrete-rhythmic patterns that displayed the same constraints as observed in the experimental data due to the synchronization properties of the nonlinear coupling of the neural units [7,56].

Hence, the first question is whether interactions between oscillatory and discrete elements are also observed in the coordination across two joints within a limb, or are the coupling constraints only observed when the discrete and rhythmic elements share the same joint? As a guide for the experiments we formulate hypothesis 1: coupling constraints between discrete and rhythmic components reside at the neural level such that control signals for rhythmic and discrete movements interact, leading to overt constraints at the kinematic output. These constraints arise at a higher level of the central nervous system and are independent of limb involvement.

The critical new aspect in multi-joint intralimb coordination, however, is that torques arise at the joints that are not only produced by muscle contractions but that also come from movements of the other joints of the segmental chain. Many studies on multi-joint coordination have highlighted the importance of intersegmental dynamics in understanding the neural control of movements. In coordinating two joints in a goal-directed movement task, the biological system has to take into account these interaction and gravitational torques, by either compensating or utilizing them. For example, Schneider and co-workers demonstrated that complex unrestrained multi-joint arm movements become smoother and faster with practice [45,46]. Underlying these kinematic effects were important changes in the intersegmental dynamics: muscle torques more effectively complemented the torques created by movements in the linked segments in accordance with Bernstein’s principle. Using the same inverse dynamics analysis for babies’ kicking movements in 3D, they showed that muscle torques counteracted and complemented gravity- and motion-dependent torques [47]. Sainburg and co-workers demonstrated that performance of the dominant and non-dominant arm differed in the degree to which muscle and intersegmental torques were related across elbow and shoulder joints [3,42]. In a comparative analysis of kinematics, torques, and EMG data, Gribble and Ostry [19] demonstrated for single- and multi-joint movements that EMG activity preceded and thereby compensated the interaction torques arising from motion of the other joint. Such anticipatory and compensatory control would require that the CNS has an internal model of the dynamics of the limb in its interactions with environmental forces.

Hence, the second question that the present study addresses is whether such intersegmental coupling effects also determine the recruitment and sequencing of different action elements. We formulate hypothesis 2: interaction

torques are the primary determinants that set the constraints on the interaction of the discrete and rhythmic action elements. The control of discrete actions is ‘cognizant’ of dynamical properties of the limb and utilizes passive torques with anticipatory control. In contrast to the referenced studies on intersegmental dynamics that investigated self-guided movements and focused on the aspect of improvement and skilled performance, the present task requires the fast execution of an integrated task. Do these control principles remain prominent when rapid reaction time movements are examined?

In order to address these questions, the present study examines a multi-joint task that involves rhythmic and discrete components in a two-joint planar movement. The task is comparable to the previous experimental tasks in that it involves the initiation of a discrete action against the background of ongoing rhythmic activity. Picking up on one of the introductory examples, we had participants ‘clean a table’. Rhythmic actions were performed by the elbow on a planar surface and a triggered discrete action of the shoulder displaced the oscillation to another target. The kinematics of joint and endpoint trajectories and the electromyographic data of the four primary flexor and extensors involved in the two-joint movement task will be examined. Inverse dynamics calculations will be performed to evaluate whether mechanical constraints are relevant in the merging of the two task elements. The discussion will address the generality of the results as seen in other task variations and the degree to which such constraints may arise at a neural or peripheral mechanical level.

2. Methods

2.1. Participants

Four graduate and two undergraduate students (two female, four male, average age: 30.2 ± 8.1 years) from The Pennsylvania State University volunteered for this experiment. They reported no motor disabilities or injuries to their upper extremities and they had no prior experience

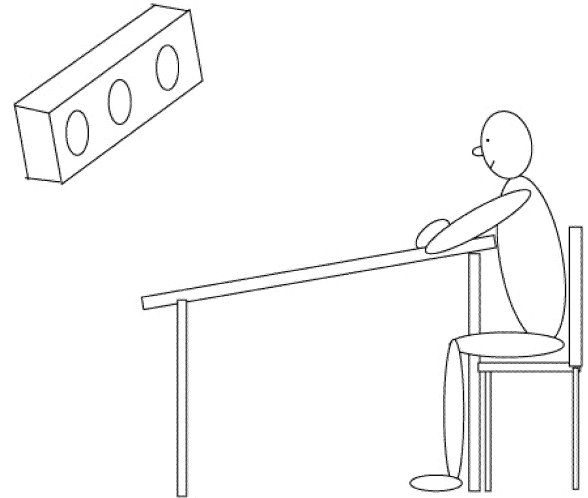


Fig. 1. Experimental set-up with the visual motion tracking system (Optotrak).

with a similar two-joint movement task in a laboratory setting. Two participants reported themselves to be left-handed. Prior to testing, all participants provided informed consent according to the Office of Regulatory Compliance of the Pennsylvania State University. Their anthropomorphic data are summarized in Table 1.

2.2. Apparatus and materials

Participants performed the arm movements on a table surface (145×80 cm) with an inclination of 11° . The height of the table was 75 cm at its lowest point and 90.6 cm at its highest point (see Fig. 1). The purpose of the incline was to facilitate readings of the limb position by the wall-mounted Optotrak data collection system (Optotrak 3020 system, Northern Digital, Waterloo, Canada). An adjustable chair was set at a height to allow for an upper arm resting position on the table such that the weight of the arm was distributed evenly over the entire arm. To reduce friction hindering the arm movements, the table was covered with sheet plastic and participants wore a tight-fitting lycra sleeve on their dominant arm that

Table 1

Anthropomorphic measurements of all six participants (P1 through P6). The length of the upper arm was measured from the lateral epicondyle to the acromion, the length of the lower arm was measured from the lateral epicondyle to the radial styloid process

Participant	Gender	Age (years)	Height (m)	Weight (kg)	Limb length (m)	
					Upper arm	Lower arm
P1	F	28	1.57	52	0.30	0.24
P2	M	21	1.78	86	0.33	0.28
P3	M	39	1.83	81	0.32	0.27
P4	M	34	1.75	72	0.33	0.28
P5	M	21	1.70	68	0.28	0.25
P6	F	38	1.70	54	0.29	0.24
Mean		30.2	1.72	68.9	0.31	0.26

extended from the wrist across the elbow to the deltoid tuberosity. To further reduce surface friction they wore a woollen glove. A wrist brace stabilized the wrist joint and avoided motions in the wrist. The participants sat with their chests leaning against the table in order to stabilize the trunk from rotation in the transverse plane. They supported themselves with their non-dominant arm resting on the table and folded by their chests. They were instructed to maintain this position during all experimental movements to minimize trunk rotation and to keep the location of the shoulder joint as stationary as possible.

Three infrared light-emitting diodes (LEDs) were attached at the following anatomical landmarks on the dominant arm: (1) radial styloid, (2) lateral epicondyle of elbow, and (3) deltoid tuberosity (Fig. 2A). The LED output was sampled at 100 Hz using the Optotrak system. Instantaneous joint angles were subsequently calculated to be the angles between the lines defined by the LED markers. The elbow angle was defined as the angle between the lines (LED1)–(LED2) and (LED2)–(LED3). The shoulder angle was defined as the angle between the line (LED2)–(LED3) and the horizontal axis that was parallel to the edge of the table. EMG activity for shoulder abduction and adduction, and elbow flexion and extension

was recorded using a Coulbourn LabLinc V system and amplified with a Coulbourn Bioamplifier (preamplification with amplifier coupler set to 0.1 Hz; gain 5 K; Model V75-01, Coulbourn Instruments, Allentown, PA, USA). The electrodes were placed on the following muscles: (1) posterior deltoid, (2) anterior deltoid, (3) brachioradialis, and (4) triceps (long head). The sampling rate was 1000 Hz. The trigger signal was recorded in the same data stream as the EMG signal.

Two small circles of 2 cm diameter were drawn on the table surface and labeled as targets T1 and T2 about which the participants were instructed to oscillate. The target positions were selected such that movements from one target to the other could be performed in a comfortable mid-region of the arm's range of motion. The targets were redrawn for each participant taking into account their specific limb segment lengths. For target T1 the shoulder and elbow angles were 90° and 100° , respectively. For T2, the shoulder angle was 130° and the elbow angle was again 100° (Fig. 2B). Hence, the discrete movement required a 40° shift in only the shoulder joint and no angular change in the elbow joint. Karst and Hasan [27,28] documented significant muscle activity in the shoulder adductors and abductors for the initiation of these angular changes. These considerations were important for the determination of the initiation time of the shoulder movement based on EMG activity in the shoulder muscles. The angular direction for the movement from T1 to T2 was 153° when measured between the direction of the forearm to the direction of the linear path between T1 and T2. The angular direction for the movement from T2 to T1 was 66° (see Fig. 2B). The absolute direction of the discrete movement from T1 to T2 was 16° , when the horizontal shoulder axis was defined as zero angle. The discrete movement from T2 to T1 had the direction of 196° . The target locations were also transformed into Cartesian coordinates, with the origin defined at the shoulder joint. Using the participants' average anthropometric lengths of upper arm and forearm and adding 0.05 m for the distance between the wrist and center of the fist to the length of the forearm, the targets had the following coordinates: T1: $x = -0.31$ m, $y = 0.36$ m; T2: $x = 0$ m, $y = 0.47$ m. The linear distance between the two targets was on average 0.33 m.

2.3. Procedure and design

The experiment was conducted in two blocks. In block 1 the participants were instructed to perform rhythmic movements about one target with their dominant arm as if they were 'cleaning the table'. The experimenter demonstrated the approximately linear movement of the hand path. At the beginning of each trial a metronome set the pace to a rate of 200 beeps per minute, equivalent to a period of 300 ms. This metronome period was selected based on preferred periods in a pilot study. The metronome was switched off after 5 s and the participants were

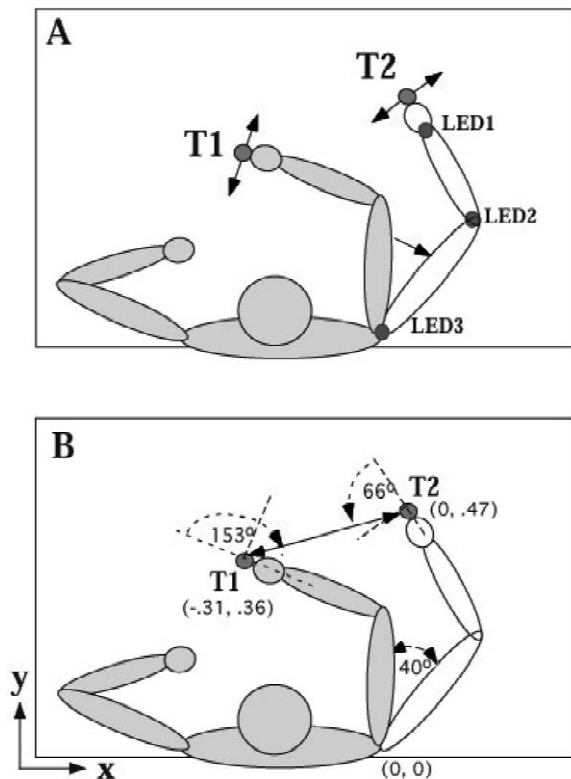


Fig. 2. Top down view onto the planar workspace with the locations of the two targets. For reasons of clarity the target dots are drawn in front of the hand. In the experiment the participants oscillated their hand on top of the dots. (A) Three LEDs were attached to the arm as indicated. (B) The angular direction of the discrete movement, the angular change in the shoulder angle, and the Cartesian coordinates of the targets are shown.

instructed to continue the same oscillatory pattern. The amplitude of the oscillation was not explicitly specified and participants found a comfortable amplitude based on the prescribed period. When one subject selected an excessive amplitude (i.e. greater than 20 cm) he/she was instructed to reduce the amplitude of oscillation. No instructions about the orientation of the rhythmic movements in extrinsic space was provided. At a random time 3–7 s later (i.e. 8–12 s into the trial), an auditory cue given by an electronic buzzer signaled to the participants to perform a discrete shift ‘as quickly as possible’ from the current target to the other target. This trigger signal occurred at a random delay with a uniform distribution. Importantly, the instruction also emphasized to ‘not stop the original oscillation’. The aim was to force participants to combine both types of actions as best as they can. After the discrete shift the participants continued to oscillate about the second target for the remainder of the 20-s trial.

Three practice trials were conducted in order for participants to find their preferred amplitude and their preferred set of shoulder and elbow motions. Note that while the angles of the two joints for each target location were uniquely determined, the orientation of the oscillatory amplitude was not specified. The oscillation made the task redundant because participants could choose different pairings of shoulder and elbow joint angles. The discrete shift between the two targets marked on the planar table surface, on the other hand, was non-redundant and could only be accomplished by an angular displacement in the shoulder joint. When the participants indicated that they felt comfortable with the task, data collection began. The metronome was turned on and the participants began oscillating about the first target. In total, 20 trials were performed within block 1: 10 trials of shifts from T1 to T2, and 10 trials of shifts from T2 to T1. The two conditions were given in randomized order. Before each trial the subject was informed at which target to start the trial. Between trials they could rest as long as they wished but typically signaled to be ready for the next trial after ~15 s.

The participants were then given 5 min of rest after which block 2 began. The same targets were employed. In contrast to block 1, the participants were now given explicit instructions regarding their joint movements. The task was to ‘perform elbow oscillations’ about the target while ‘keeping the shoulder joint stationary’. Upon hearing the random trigger signal, the participants were instructed to ‘perform a discrete shoulder shift as quickly as possible from target to target without stopping the elbow oscillation’. Three practice trials were again performed to allow the participants to become comfortable with the explicit task requirements. Twenty trials were performed for block 2: 10 trials of shoulder shifts from T1 to T2, and 10 trials of shoulder shifts from T2 to T1. The two conditions were again randomized within the block of 20 trials. The number of trials was that which could be done in one session without incurring fatigue in the participants. The

duration of the entire experiment was ~60 min. Participants could rest between trials to avoid fatigue if they wanted.

2.4. Data reduction and dependent measures

The raw position data were filtered using a 6th order Butterworth filter with a cut-off at 40 Hz. Subsequently, joint angles were calculated from the x - y locations of the optically recorded data. Full elbow extension was defined as 180° with flexion decreasing the angle, full shoulder abduction was defined as 180° with adduction decreasing the angle. The EMG signals were analog bandpass filtered with cut-offs at 13 and 1000 Hz and sampled at 1000 Hz.¹ The digitized signal was subsequently full-wave rectified and digitally filtered applying a 6th order low-pass Butterworth filter with a cut-off frequency of 70 Hz.

2.4.1. Steady state periods and amplitudes

The first step in assessing the kinematics of the participants’ performance was to parse the joint angle trajectories into cycles. For both shoulder and elbow joint angle trajectories, the cycle periods were calculated as the difference between successive maxima t_E and t_S . The subscripts E and S refer to elbow and shoulder, respectively. Cycle amplitudes were calculated as the difference between maxima and minima of the oscillatory signals. The steady state behavior of each joint trajectory before and after the discrete shift was characterized by the mean period and mean amplitude of its oscillation calculated over five cycles directly preceding the discrete trigger signal, $T_{E, pre}$, $A_{E, pre}$, and five cycles after the discrete shift $T_{S, post}$ and $A_{S, post}$. The post-discrete mean was calculated over cycles 4 to 8 after the transition to eliminate transient effects.

2.4.2. EMG timing

To find a robust estimate of the timing of the rhythmic muscular activity, the center of mass (COM) of each burst was calculated. To do this, the EMG signals were parsed into cycle segments at the time of the maxima or minima of the elbow joint trajectory. Successive minima of the elbow signal were used to partition the EMG signals of the anterior and posterior deltoids and the triceps (see Fig. 3). Due to different relative timing of activity among the muscles, successive peaks of the elbow signal served to partition the activity of the brachioradialis. Within each segment, the total area of the burst was calculated by using

¹The amplifier hardware constrained the analog low-pass filter settings to 1000 Hz. In pilot experiments it was verified that there was very little frequency content in the signal above 400 Hz so that the sampling frequency could be kept at 1000 Hz without introducing aliasing effects according to Nyquist’s sampling theorem. Additionally, the reliability of the onset detection was evaluated in pilot trials with different analog filters and sampling frequencies, yielding these settings the best choice.

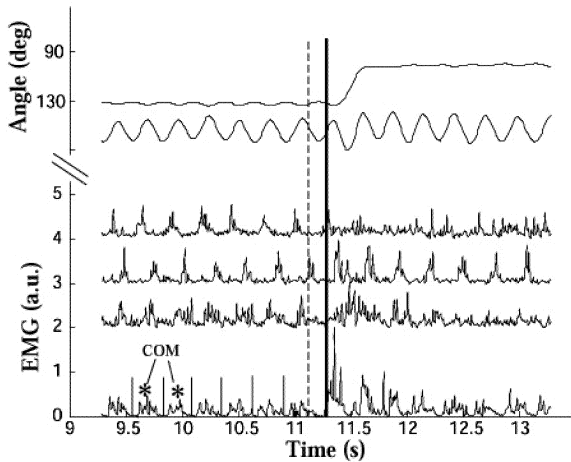


Fig. 3. Segment of the time series of the two angle trajectories of the shoulder (top) and elbow joint (second from top) in an abduction trial. The EMG traces of the four elbow and shoulder muscles are shown in the order from top to bottom (arbitrary units): brachioradialis, lateral head of triceps, anterior deltoid, posterior deltoid. The dashed vertical line indicates the time of the trigger signal, the solid vertical line indicates the time of the super-threshold activity of the discrete agonist, for the shown abduction trial, the posterior deltoid.

the trapezoid method. The COM was then identified at the point in time where the integral reaches half of its total value. The times of the successive COMs within each trial were numbered with respect to the trigger signal: the EMG bursts immediately following the trigger were labeled with positive integers, e.g. COM_1 , COM_2 . COMs preceding the trigger were identified with negative integers, where the last burst before the discrete movement started as COM_{-1} . The temporal difference between the successive COM_i s was used to calculate the mean periods in the EMG activity, T_{EMG} .

2.4.3. Relative phase

To assess the relative timing of muscle activity between the four measured muscles studied, three pairwise relative phases between the brachioradialis and each of the other muscles were calculated. The brachioradialis was chosen as the reference signal because it exhibited the most pronounced burst pattern. For each trial, the time differences between the COM_i of the brachioradialis and the COM_j of the other three muscles immediately following in time were determined. The time differences between all bursts of a pair of signals preceding the discrete shift were averaged for each trial. This mean value was then divided by the mean EMG period of the brachioradialis, T_{EMG} , and multiplied by 2π to convert the time difference to a phase. Specifically, the relative phase between the triceps and the brachioradialis $\phi_{rel,tri}$ was defined as:

$$\phi_{rel,tri} = \frac{2\pi}{n} \sum_{i=1}^n \frac{COM_{-i,tri} - COM_{-i,br}}{T_{EMG}}$$

where n is the number of COMs observed in the brach-

ioradialis before the discrete initiation. To calculate $\phi_{rel,ant}$ and $\phi_{rel,post}$ the time of the COMs of the anterior and posterior deltoids was substituted for the COM of the triceps in the equation.

2.4.4. Onset of the discrete movement

The EMG signal of the major agonist muscle, anterior deltoid for shoulder adduction and posterior deltoid for abduction, served as the basis for locating the beginning of the discrete movement. For the shoulder angle changes of 40° significant muscle activity could be expected for the initiation of shoulder adduction and abduction [27,28]. To determine the time of the discrete onset t_{EMG} the routine first identified the highest peak of the signal after the trigger which unambiguously corresponded to the peak associated with discrete movement. Then, the routine identified the data sample preceding this peak that was larger than 15% of the peak amplitude and marked this as the event onset t_{EMG} (see Fig. 3). Subsequently, all calculated onset times t_{EMG} of each trial were checked by eye by an experienced observer and obviously false detections were adjusted. Trials where t_{EMG} could not be determined in an unambiguous manner were excluded from further analysis. Across all subjects 2% of all trials had to be excluded. This criterion for detection of initiation was consistent with previous related studies that investigated the initiation of a discrete movement against oscillatory background actions.² We also checked whether an earlier attenuation of activity in the antagonist could be a more appropriate indicator for the initiation of a discrete action ('Hufschmidt effect'), but no consistent pattern could be identified (see also Footnote 1 in Ref. [57]). Even if some attenuation in the antagonist was discernible, this posed a challenge to define a reliable criterion for marking the onset. Hence, in accord with similar studies on two-

²The objective detection of a specific motor response in surface EMG signals is a recalcitrant problem, particularly when the signal contains activation from a secondary motor task. Many computerized algorithms have been developed with the goal to detect events online in a reliable and replicable fashion in a large number of trials. Such methods can operate in the time domain, as the routine that was applied for the present data, or in the frequency domain. The threshold can be defined for a single sample, as in the present routine, or for an average value within a moving window. The threshold can be fixed, proportional, as in the present case, or adaptive. Event detection and determination of onset time can also employ a model-based detection of parameter changes. This method detects events in a highly accurate manner but, in turn, is dependent on knowledge of the underlying processes of the signal captured by the model. For an overview over methods and a model-based algorithm see Refs. [50,52].

While many sophisticated algorithms have been proposed and compared in the literature, their critical evaluation still does not substitute the critical intuitive check by an experienced observer. As our experiment did not require online detection and did not have an excessive number of trials we used the relatively simple algorithm combined with the evaluation by the experimenter. In related work, we compared the onset detection by two experienced experimenters. The discrepancy between two evaluations of ~400 trials was of the order of 10 ms [57].

joint movements, movement initiation was defined by increased activity in the agonist [27].

The timing of the discrete onset was then converted into a phase ϕ_{EMG} . Two reference signals were used: firstly, ϕ_{EMG} was calculated with respect to the rhythmic timing of the same muscle that initiated the discrete movement:

$$\phi_{EMG} = 2\pi \left(\frac{t_{EMG} - COM_{-1}}{T_{EMG}} \right).$$

The COM_{-1} and T_{EMG} of the anterior or posterior deltoid were used to calculate ϕ_{EMG} . Further, a kinematic onset phase ϕ_{KIN} was also calculated by relating t_{EMG} to the joint angle of the oscillation. The calculation of ϕ_{KIN} was similar in form to that of ϕ_{EMG} :

$$\phi_{KIN} = \left(\frac{t_{EMG} - t_p}{T_{E,pre}} \right) 2\pi$$

where t_p is the peak in the elbow joint signal prior to t_{EMG} . Therefore, $\phi_{KIN} = 0$ corresponds to maximum extension of the elbow joint trajectory.

2.4.5. Phase shift

To assess the perturbation of the rhythmic activity performed in the elbow by the discrete shoulder movement, the temporal shift of the oscillation after the discrete movement was calculated. The phase shift $\Delta\phi$ was computed on the basis of the kinematic position signal of the elbow as:

$$\Delta\phi = 2\pi \frac{t_{P,3} - t_{P,-1} - 3T_{E,pre}}{T_{E,pre}}$$

where $t_{P,-1}$ refers to the time of the elbow flexion peak directly before the onset of the discrete movement. $t_{P,3}$ refers to the time of the third peak after the onset of the discrete movement. $T_{E,pre}$ is the average period of the elbow oscillation prior to the trigger signal. In short, $\Delta\phi$ captures the average phase shift calculated at the third peak after the discrete event. We chose to capture $\Delta\phi$ three cycles after the discrete event to avoid local perturbations to influence the estimate. A negative $\Delta\phi$ indicates a shortening of the cycles during the discrete event. Conversely, positive values of $\Delta\phi$ manifest that cycles were lengthened.

2.4.6. Reaction time

Premotor reaction time was measured as the time between the onset of the auditory stimulus and the time of the super-threshold EMG activity.

2.4.7. Peak discrete velocity

Peak velocity of the discrete shoulder movement was determined as the maximum velocity between t_{EMG} and the end of the trial. Peak velocity in the discrete transition was unambiguous to detect.

2.4.8. Joint torques

For each trial, the instantaneous torques acting at each joint were calculated. In multi-joint movements, torques arise not only from forces exerted on the limb segments by muscles and forces due to gravity, but also from forces that moving segments exert on each other. We partitioned these torques into four categories: net torque T_N is defined as the inertial torque acting at each joint, equal to the sum of all positive and negative torque components acting at a joint. Interaction torques T_{IA} are defined as those torques acting at a given joint due to motion of the other segment (Coriolis, centripetal and coupling torques). Gravitational torques T_G are passive torques resulting from gravity acting on the center of mass of each segment. Although, the task was performed on a planar surface, the inclination of this table top introduced small gravitational torques. Muscle torque T_M is the torque that has to be produced primarily by muscle forces. Note, however, that one cannot interpret muscle torque directly as muscle commands because there are also passive effects of soft tissue deformation. In addition, the force generated by a muscle is dependent on muscle length, speed of muscle length change, and activation history. The equations for calculating joint torques from the mechanical characteristics of the limb and the recorded kinematic trajectories were based on a two-link arm moving in a plane [24,62]:

$$T_{E,N} = \ddot{\theta}_E (I_E + m_E l_{E1}^2) \quad (1)$$

$$T_{E,IA} = -\ddot{\theta}_S [I_E + m_E (l_{E1}^2 + l_S l_{E1} \cos \theta_E)] - \dot{\theta}_S^2 (m_E l_S l_{E1} \sin \theta_E) \quad (2)$$

$$T_{E,G} = m_E l_{E1} g \cos \alpha \cos (\theta_E + \theta_S) \sin \alpha \quad (3)$$

$$T_{E,M} = T_{E,N} - (T_{E,IA} + T_{S,G}) \quad (4)$$

$$T_{S,N} = \ddot{\theta}_S [I_S + m_S l_{S1}^2 + I_E + m_E (l_S^2 + l_{E1}^2 + 2l_S l_{E1} \cos \theta_E)] \quad (5)$$

$$T_{S,IA} = -\ddot{\theta}_E [I_E + m_E (l_{E1}^2 + l_S l_{E1} \cos \theta_E)] + \dot{\theta}_E^2 (m_E l_S l_{E1} \sin \theta_E) + \dot{\theta}_S \dot{\theta}_E (2m_E l_S l_{E1} \sin \theta_E) \quad (6)$$

$$T_{S,G} = m_S g l_{S1} \cos \alpha \cos \theta_S \sin \alpha + m_E g [(l_S^2 + l_{E1}^2 + 2l_S l_{E1} \cos \theta_E)]^{1/2} \cos \alpha \cos \left[\theta_S + \arcsin \left(\frac{l_{E1}}{(l_S^2 + l_{E1}^2 + 2l_S l_{E1} \cos \theta_E)^{1/2}} \sin \theta_E \right) \right] \sin \alpha \quad (7)$$

$$T_{S,M} = T_{S,N} - (T_{S,IA} + T_{S,G}) \quad (8)$$

θ_E , θ_S are the exterior angles of the elbow and shoulder, and the dots denote time derivatives. Note that the definition of joint angles where full extension corresponds to zero angles is common in the respective literature and contrast with the joint angle definition above which is anatomically motivated. The symbols I , m and l denote segment rotational inertia, mass and length of the limb segments, respectively. The subscripts E1 and S1 to the lengths denote the distance to the center of masses of the two limb segments, measured from proximal to distal. The angle α is the inclination angle of the table that was 11° . The gravity constant is 9.81 m/s^2 . To determine the parameters of the participants' limbs, anthropometric measurements were taken and are summarized in Table 1. For the upper arm this length was adjusted to account for the biomechanical length which is 10% shorter than the anatomical length. Mass, moment of inertia, and distances to the center of masses were estimated using regression equations developed on the basis of cadaver measurements [62].

To characterize the typical steady state behavior for individual participants in each experimental condition, mean single-cycle torque profiles were calculated for $T_{S,IA}$, $T_{S,M}$, $T_{S,N}$ and $T_{S,G}$ as well as $T_{E,IA}$, $T_{E,M}$, $T_{E,N}$ and $T_{E,G}$. For each trial, each of the eight torque profiles was divided into cycles at the points of maximum elbow extension. The torque values of each cycle were then rescaled in time to a standard number of samples (the trial mean cycle length) using cubic spline interpolation. The torque values of all resampled cycles were then averaged at each point in time, yielding a single mean cycle pattern for the trial's average cycle. To assess the behavior of each participant in the experimental conditions, the mean profile for each torque component was calculated per block and direction of the discrete transition, again by first resampling the individual trial mean profiles of all trials in a block to a standard number of samples and then averaging at each point. We also quantified the contribution of interaction torque during the accelerating segment of the discrete movement by calculating its integral, i.e. its impulse. Intervals at which T_{IA} acted in the same direction as the discrete movement were considered positive. Intervals in which the T_{IA} acted in the opposite direction were considered a negative impulse. To summarize this effect, the total number of trials was counted in which the impulse aids the movements and divided by the total number of trials.

3. Results

3.1. Kinematic and EMG analysis

A first impression of the participants' performance can be obtained from Fig. 4 that shows one trial's trajectory from a top-down perspective onto the x - y plane. The selected trial was taken from block 1 where the participant

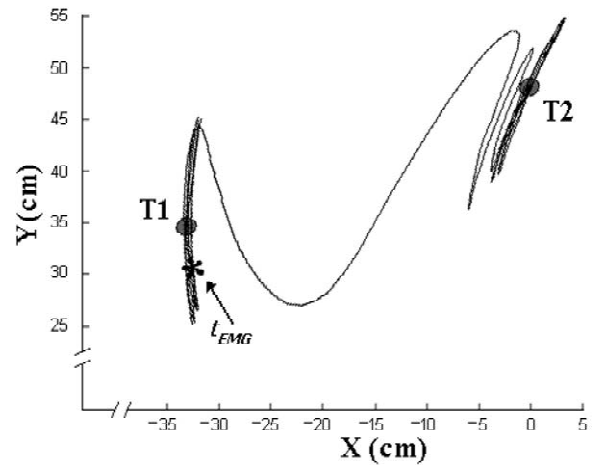


Fig. 4. Single trial trajectory from block 1 where no instruction about joint movement was given. The discrete movement was initiated at target 1 (T1) and involved a shoulder abduction movement to target 2 (T2). The star depicts the instant of the discrete movement's onset as determined from the EMG signal.

was naive with respect to the joint involvement. He began the oscillatory movement at T1 and shifted to T2 with a shoulder abduction. The star in the left oscillatory segment illustrates the instant of the initiation of the discrete movement as determined on the basis of supra-threshold EMG activity in the posterior deltoid. This trial exemplifies the most frequent initiation of the discrete shoulder movement at time $t_{EMG} \sim 1/4$ of a cycle after maximal elbow flexion. As maximum elbow flexion is defined as π rad in the ongoing oscillatory movement this corresponds to a ϕ_{KIN} of $3/2\pi$ rad (see histogram of ϕ_{KIN} in Fig. 7). The oscillatory amplitude was ~ 15 cm, the discrete movement extent was ~ 27 cm in the x - y plane. The curved transition trajectory shows that the oscillations were indeed continued during the discrete movement in accord with the instructions.

Fig. 3 shows a time series of the joint angle trajectories together with the four EMG signals of a shoulder abduction trial, again selected from block 1. The dashed vertical line depicts the time of the trigger signal, the solid vertical line shows the time of the discrete initiation determined by the supra-threshold activity of the posterior deltoid. Despite the 'open' task instruction—the direction of the oscillation was not prescribed—the rhythmic actions were largely confined to the elbow joint, while the discrete displacement was performed in the shoulder joint. While the translation necessarily had to be executed in the shoulder joint, the fact that only the distal joint performed the oscillation was not stringent in this naïve task condition. The initial EMG burst in the posterior deltoid, plotted as the bottom signal, is followed by a pronounced burst in the antagonist anterior deltoid, shown above, and completed by another agonist burst in the posterior deltoid in line with the common triphasic pattern found in fast discrete movements. In addition, pronounced rhythmic

activity is observed in the two shoulder muscles throughout the trial. This is most likely necessary to maintain a stationary shoulder joint position in the face of the interaction torques produced by the elbow movements. Note also, that the EMG patterns directly following the discrete movements were typically more noisy, probably due to the perturbation from the inserted discrete movement. Therefore, this part of the EMG time series was not included in the data analyses.

3.1.1. Steady state oscillations

A first focus was directed at the steady state behavior before and after the discrete shift. According to the instructions, the same oscillation amplitude and frequency should be maintained throughout the entire trial. However, were there changes in the oscillation due to the insertion of the discrete change in the workspace location or due to the perturbation? A second question was what kind of joint angle combinations did participants employ in the naïve performance in block 1 compared to the instructed performance in block 2? To address these questions, the kinematic parameters amplitude and period were analyzed in a repeated-measures analysis of variance with the factors block (naïve vs. instructed), direction (T1–T2 vs. T2–T1), and the average behavior before and after the discrete transition (pre vs. post). For each participant, the mean amplitudes and periods during the steady state intervals before and after the transition were computed, separately for each joint angle trajectory. Subsequently, participant averages were computed across the 10 trials in each transition direction, again separately for each block (see Table 2). Four three-way 2 (block) × 2 (direction) × 2 (pre/post) ANOVAs were performed separately for shoulder and elbow joints and amplitudes and periods.

Neither of the two ANOVAs on amplitudes yielded significant results. The mean amplitudes at the elbow, $A_{E,pre}$ and $A_{E,post}$ across all trials was 19.5° , with participant means ranging between 12.6 and 27.5° . Note that there were no explicit amplitude targets and accuracy was not a factor. At the shoulder, $A_{S,pre}$ and $A_{S,post}$, the overall average was 4.0° , with participants' means ranging between 1.7 and 6.9° (see Table 2). With respect to the first

question, this result shows that there were no significant changes in the amplitude from the pre-discrete to the post-discrete interval, implying that the mean joint angle amplitudes were not perturbed by the transition event, neither in the shoulder nor in the elbow. With respect to the second question, the comparison between the instructional conditions, this persistence in the amplitude was seen similarly in both instruction conditions. This means that participants performed the oscillatory task mainly by elbow rotations in the naïve condition, similar to the instructed condition, even though the task was unspecified with respect to joint recruitment.

The same two ANOVAs performed on period detected a significant main effect for block in the elbow joint, $F(1,5)=23.47$, $P<0.01$, indicating that the average period of the elbow oscillation was slightly shorter in the instructed condition (289 ms) than in the naïve condition (297 ms). In the shoulder joint this effect failed to reach significance. However, there was a significant interaction between instructional condition and pre/post segment, $F(1,5)=7.39$, $P<0.05$. This indicated that, while T_S decreased from the pre- to post-transition segment in block 2, T_S did not change in block 1. There was a trend for a shortening of the period that did not reach significance. The mean amplitudes and periods during the steady state rhythmic segments are summarized in Table 2. In sum, the analyses on both amplitudes and periods show that participants maintained the oscillation throughout the trial across the discrete transition. The two instructional conditions did not show any striking differences with the exception of a small difference in the period of the elbow oscillations.

3.1.2. Relative phase of rhythmic EMG activity

As illustrated in the times series in Fig. 3 both shoulder muscles were rhythmically active even when the shoulder joint was relatively stationary. Hence, relative phase between pairs of muscles was calculated during steady state performance for the segment prior to the transition. The maximum activity of the brachioradialis served as the reference phase zero for all three pairwise relative phases. Fig. 5 displays the mean values across the 10 repetitions

Table 2

Kinematic parameters of the rhythmic movements of shoulder and elbow trajectories before (Pre) and after (Post) the discrete transition for both instructional conditions (block 1 and block 2). The left entry in each cell lists the mean amplitude in degrees over 10 trials per participant. The right entry is the mean period in milliseconds over 10 trials per condition of each participant

Participant	Block 1				Block 2			
	Shoulder		Elbow		Shoulder		Elbow	
	Pre	Post	Pre	Post	Pre	Post	Pre	Post
P1	2.3/310	3.2/333	24.0/310	23.1/315	1.8/305	2.1/318	24.1/308	20.9/305
P2	3.4/312	3.9/309	20.4/312	18.9/295	2.2/319	4.1/307	23.2/300	14.6/290
P3	3.1/319	4.2/330	26.7/318	25.7/316	2.1/320	2.3/330	31.2/305	26.3/308
P4	2.3/294	3.2/306	21.6/295	21.9/297	2.2/282	3.4/296	19.0/282	20.0/284
P5	2.5/276	2.3/275	9.2/270	13.1/268	1.0/275	1.2/262	15.3/261	12.9/265
P6	1.9/288	1.9/292	15.9/289	14.5/280	1.8/290	1.9/284	16.1/290	14.9/274

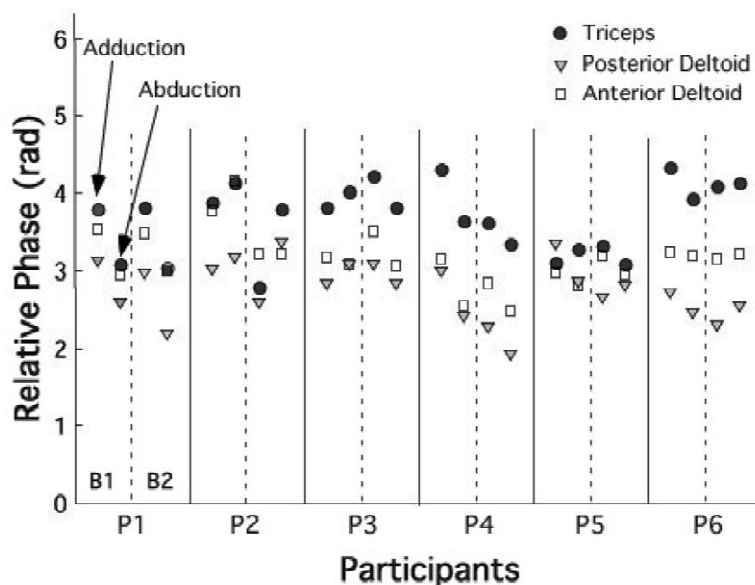


Fig. 5. Mean relative phase of three pairings of muscles: for the long head of the triceps, the anterior and posterior deltoid, the brachioradialis served as reference phase zero. For each participant the mean values are calculated within each block and direction separately. For each participant, the first two values are determined for block 1, the second two values are determined for block 2. Within each block the first value is determined for the adduction trials, where the pre-transition steady state oscillation occurs around target 2. The second values belong to abduction trials with the pre-transition oscillation around target 1.

per condition for each of the six participants. For all participants, triceps and brachioradialis showed an anti-phase relationship as to be expected from the required alternating flexion–extension pattern in the elbow. The relative phases in both anterior and posterior deltoid similarly formed a relation close to antiphase with the brachioradialis. This, in turn, meant that both shoulder muscles were activated synchronously implying co-contraction at the shoulder muscles. Triceps and brachioradialis appeared to have a slight phase difference compared to the shoulder muscles, showing a relative phase slightly larger than π rad.

3.1.3. Onset of the discrete movement

A pivotal question of the previous experiments on the combination of discrete and rhythmic movements was whether the initiation of the discrete movement was constrained by the ongoing oscillatory activity. As this measure is regarded central, two different phases were calculated: firstly, ϕ_{EMG} was calculated by projecting t_{EMG} into the EMG activity of the respective agonist for the discrete movement, posterior or anterior deltoid. Secondly, t_{EMG} was projected into the ongoing elbow trajectory to determine ϕ_{KIN} .

To determine whether the shoulder movement initiation was constrained by the EMG activity in the shoulder muscles, four histograms were plotted separately for the two instructional conditions and the two transition directions. Unimodal distributions were found in the two abduction conditions, whereas the adduction conditions did not differ from a uniform distribution. Also, the two

instructional conditions did not produce any difference in their distributions. Hence, trials from both blocks were pooled together for the statistical analysis. The histogram of ϕ_{EMG} in Fig. 6A clearly shows a preference for initiation around 0 or 2π rad and a less frequent occurrence at π rad. A χ^2 -test confirmed this observation with a significant difference from a uniform distribution, $\chi^2 = 27.48$, $df = 9$. This means that the shoulder movement tended to be initiated when the rhythmic burst that was observed during the pre-transition steady state would have occurred. The adduction trials, on the other hand, shown in Fig. 6B, did not differ from a uniform distribution.

The same analyses were performed for the frequency distributions of ϕ_{KIN} in the four experimental conditions. The pattern of results was identical to the ones for ϕ_{EMG} , with χ^2 values that differed from the respective values on the ϕ_{EMG} comparisons by maximally 1.3 units. Fig. 7A and B displays the two histograms for the pooled adduction and abduction trials. Again, a definite mode could be observed in the distribution of ϕ_{KIN} in abduction trials, located in the later half of the cycle at $\sim 3\pi/2$ rad (panel A), $\chi^2 = 20.19$, $df = 9$. The phase difference compared to ϕ_{EMG} is due to the fact that maximal flexion in the kinematic trace is time-delayed with respect to the flexor burst. In adduction trials (panel B) the distribution is amodal, and not statistically different from a uniform distribution, $\chi^2 = 11.71$, $df = 9$, reflecting that the rhythmic movement did not act as a constraint upon the discrete shifts in this direction. The distributions of ϕ_{KIN} found in adduction trials differed from those found in abduction trial, $\chi^2 = 39.12$, $df = 9$. In sum, comparing the distribu-

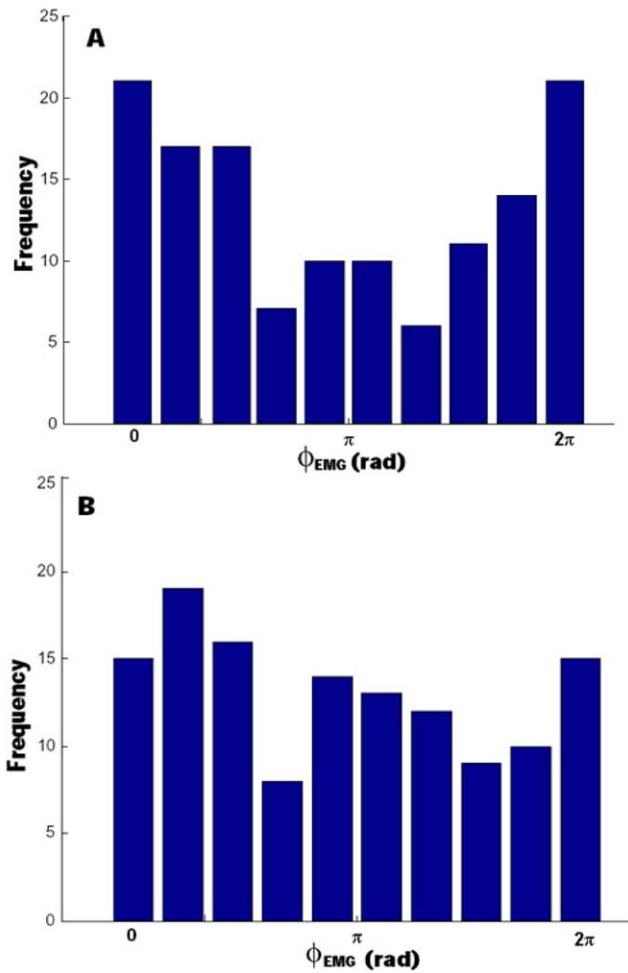


Fig. 6. Frequency distributions of the phase of the discrete movement onset determined with respect to the EMG activity of the posterior deltoid. (A) All trials involving shoulder abduction pooled across both instructional conditions. (B) All trials involving shoulder adduction pooled across both instructional conditions.

tions of ϕ_{EMG} and ϕ_{KIN} two main findings can be stated: (1) in the abduction trials there is a clear tendency toward clustering the onset to a subset of phases that is absent in the adduction trial. (2) The modal distribution of ϕ_{EMG} is less pronounced than the distribution of ϕ_{KIN} .

3.1.4. Reaction time

The time between the trigger signal and the supra-threshold EMG activity also served to calculate pre-motor reaction time. Conducting the same 2 (block) \times 2 (direction) ANOVAs on the mean reaction times across 10 trials per condition, no differences could be identified. The average reaction time across all trials was 312 ms, with individual participants ranging between 210 and 522 ms. There was a tendency for the reaction times to be shorter in the abduction direction, but given high variability across participants, no significance was obtained. There was no tendency when the two instructional conditions were compared. The reaction times of each participant, pooled

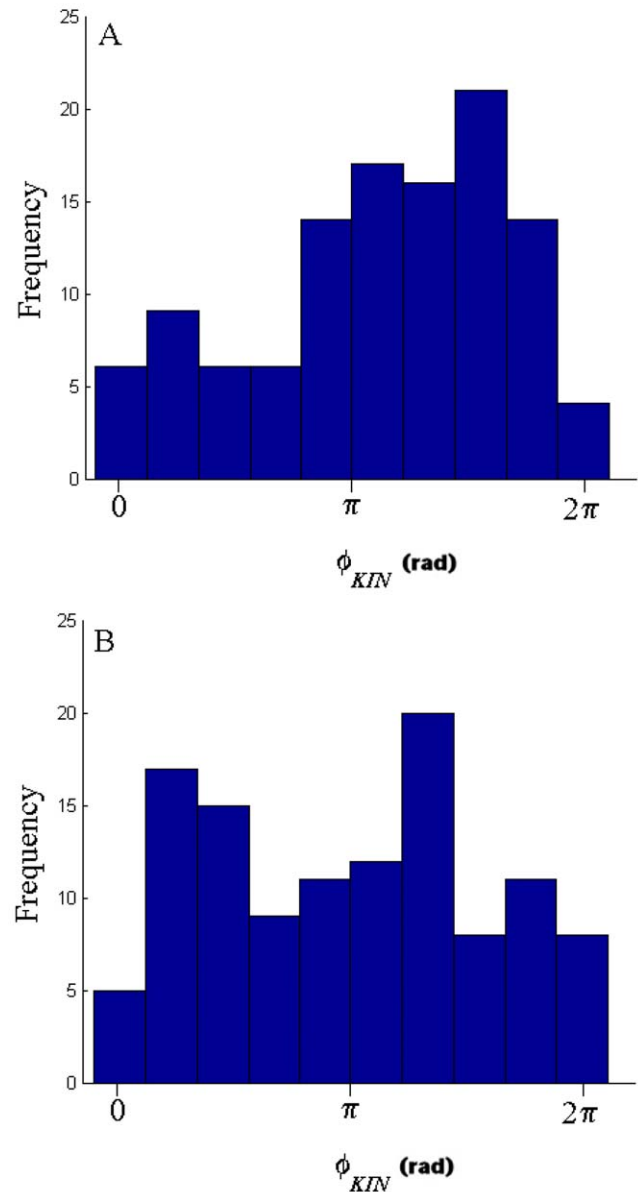


Fig. 7. Frequency distributions of the phase of the discrete movement onset, determined in terms of the phase of the elbow joint rotations. (A) All trials involving shoulder abduction pooled across both instructional conditions. (B) All trials involving shoulder adduction pooled across both instructional conditions.

over the two instruction conditions, were also regressed against the phase of the trigger signal but no systematic modulation was manifest.

3.1.5. Phase shift

To estimate the degree of perturbation of the ongoing rhythmic activity by the discrete movement, the phase shift $\Delta\phi$ was examined. Firstly, we scrutinized whether $\Delta\phi$ depended on the phase of the trigger signal or the discrete onsets ϕ_{EMG} and ϕ_{KIN} . However, no systematic modulation could be discerned. Hence, average values of $\Delta\phi$ were calculated for each participant across the 10 trials in each

experimental condition and submitted to a 2×2 ANOVA. No systematic dependencies between experimental conditions were identified. Therefore, all $\Delta\phi$ values for all participants were pooled in the histogram shown in Fig. 8. The mean $\Delta\phi$ value was -1.08 rad with a standard deviation of 2.11 rad. Note, that negative values captured the case where the cycle(s) coincident with the discrete movement shortened. Scrutinizing the mean $\Delta\phi$ value of each participant computed for each block and direction separately, only four of 24 means were greater than zero. Participants' mean $\Delta\phi$ values computed across all conditions ranged between -0.36 and -2.05 rad.

3.1.6. Discrete movement

Peak velocity was used as one descriptor for the discrete movement. As above, averages across 10 repetitions per condition were entered into an ANOVA. No significant differences were revealed between the two movement directions or instructions ($P > 0.06$). The overall average peak velocity was $177^\circ/\text{s}$.

3.2. Joint torque analysis

3.2.1. Joint torques during steady state

Having identified that there were systematic kinematic and electromyographic constraints from the rhythmic onto the discrete movement in the shoulder abduction, the next question was whether these phase preferences were coincident with phases where torques were assisting the initiation of the discrete movement. A first focus of

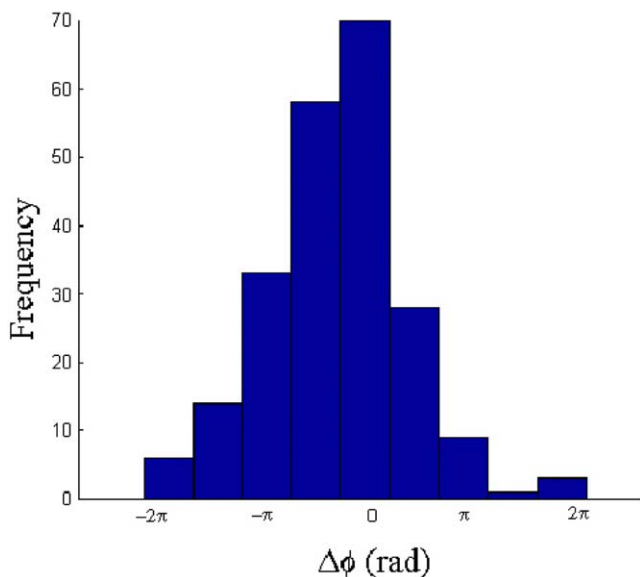


Fig. 8. Frequency distribution of phase shifts $\Delta\phi$ in the elbow joint trajectory. The data of all participants and all conditions are pooled. Negative $\Delta\phi$ express a phase advance or shortening of the cycle due to the discrete perturbation, positive values indicate a phase delay or lengthening of the cycle.

analysis was on the torque pattern during the rhythmic steady state segment preceding the discrete movement. Which phase would be predicted to be the preferred moment of onset from a torque optimization perspective? The average torque patterns for muscle, interaction, gravitational, and net torques were computed and plotted against the average cycle phase of the elbow trajectory. Fig. 9 shows the patterns of participant 1 as an example. Prior to this computation we had scrutinized the time series of the torque profiles and found sufficient consistency within and across trials of one condition to warrant such averaging. Ten trials per direction condition were averaged for shoulder and elbow separately. Zero rad corresponds to maximum extension, π rad to maximum flexion of the elbow joint. Positive torques represent torques that aid adduction in the shoulder and flexion in the elbow. Comparison of the naïve with the instructed condition did not show any differences, a result that was already foreshadowed in the analyses of steady state kinematics. Hence, Fig. 9 only shows the naïve condition.

Fig. 9A and B shows the shoulder torques during oscillations around the targets T1 and T2, respectively. For the oscillations around T1 (which precedes a shoulder abduction) this participant shows a pattern in which interaction torques oppose the muscle torque. Muscle torques, however, show greater absolute magnitudes so that the shape of the net torque track the muscle torque. This pattern signals that the interaction torques are over-compensated and the shoulder joint oscillates in phase with the elbow joint (simultaneous flexion and extension in elbow and shoulder). The interaction torques are positive in the middle segment of the elbow cycle which signals that adduction is assisted, while around maximal elbow flexion and extension, the interaction torques are negative, favoring abduction. This general pattern is similar also for the adduction trials, begun with oscillations around T2, only the interaction torques are slightly more modulated. While this latter difference is not generic across participants, the gravitational torque is always markedly greater than zero in the oscillation around T2, in contrast to the close to zero effect for oscillation around T1. This implies that shoulder adduction is generally facilitated by gravity throughout the entire cycle. Hence, if the discrete movements utilize interaction torques, movement initiation in adduction trials should be favored at ϕ_{KIN} values between $\pi/2$ and $3\pi/2$ rad. In abduction trials ϕ_{KIN} should be between $3\pi/2$ and $\pi/2$ rad. Conversely, if existent muscle torques were exploited, then the remaining segment of the cycle should be favored.

Fig. 9C and D shows the torque profiles at the elbow. Interaction torques are small and only slightly modulated during the cycle, affirming previous observations that shoulder amplitudes are small, even though this trial is from the naïve block where the participant did not receive any instructions concerning shoulder involvement. Positive interaction torque indicates that movements at the shoulder

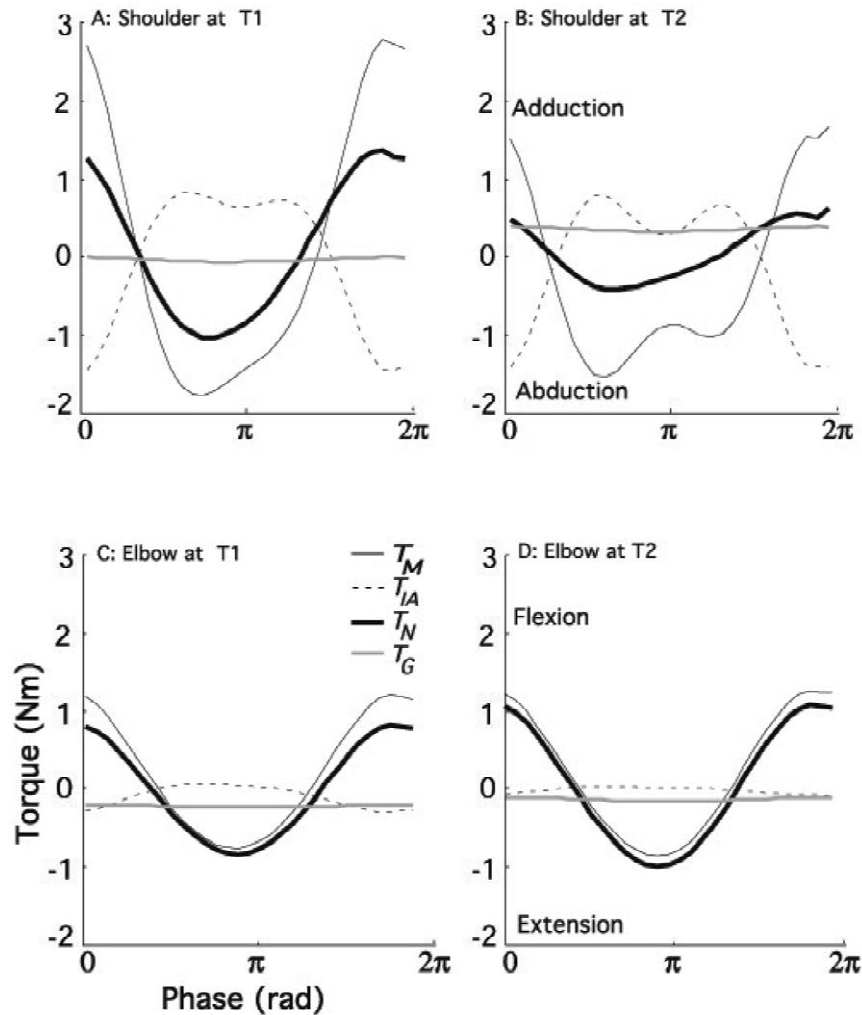


Fig. 9. Mean torque profiles during the steady state segment prior to the discrete transition. These profiles are representative for participants 1, 3, and 5. The reference phase was taken from the elbow joint cycle where 0 rad corresponds to maximum extension, π rad refers to maximum flexion. (A) Torques at the shoulder for the abduction trials where the steady state oscillation is performed around target 1. (B) Torques at the shoulder for the abduction trials where the steady state oscillation is performed around target 2. (C) Torques at the elbow for the abduction trials where the steady state oscillation is performed around target 1. (D) Torques at the elbow for the abduction trials where the steady state oscillation is performed around target 2. Muscle torque, interaction torque, net torque and gravitational torque are denoted by different lines shown in panel C.

assist flexion at the elbow. As interaction torque has the opposite sign to the net torque, it is opposing the actual movement. The muscle torque parallels the net torques indicating that the movement is produced primarily by this muscle torque, probably to a large degree by active muscle contraction. Gravitational torques were relatively small for oscillations around both targets, although they slightly facilitated elbow extension, especially in elbow oscillations around T1. With respect to the discrete shoulder movement no direct hypotheses can be stated from elbow torques.

This participant's torque profile is representative for two other participants (P3, P5). A second group of three participants (P2, P4, P6) performed with torque profiles in the shoulder joint that displayed a different relation between net torque and interaction torque. While the first

group can be characterized by the observation that muscle torques overcompensate the interaction torques, the second group showed net torque patterns that mirrored the interaction torques. The torque profiles of one participant of this second group are displayed in Fig. 10. Hence, while there were (active) muscle contractions, they did not fully cancel the effect of the interaction torques. This separation of behaviors between participants into two classes was consistent across all four experimental conditions. Note, that there was no mapping between the right-handed and the left-handed participants with either pattern. Scrutinizing elbow torque profiles, interindividual differences were less pronounced as the shoulder movements always had relatively small amplitudes and the interaction torques at the elbow therefore remained fairly small.

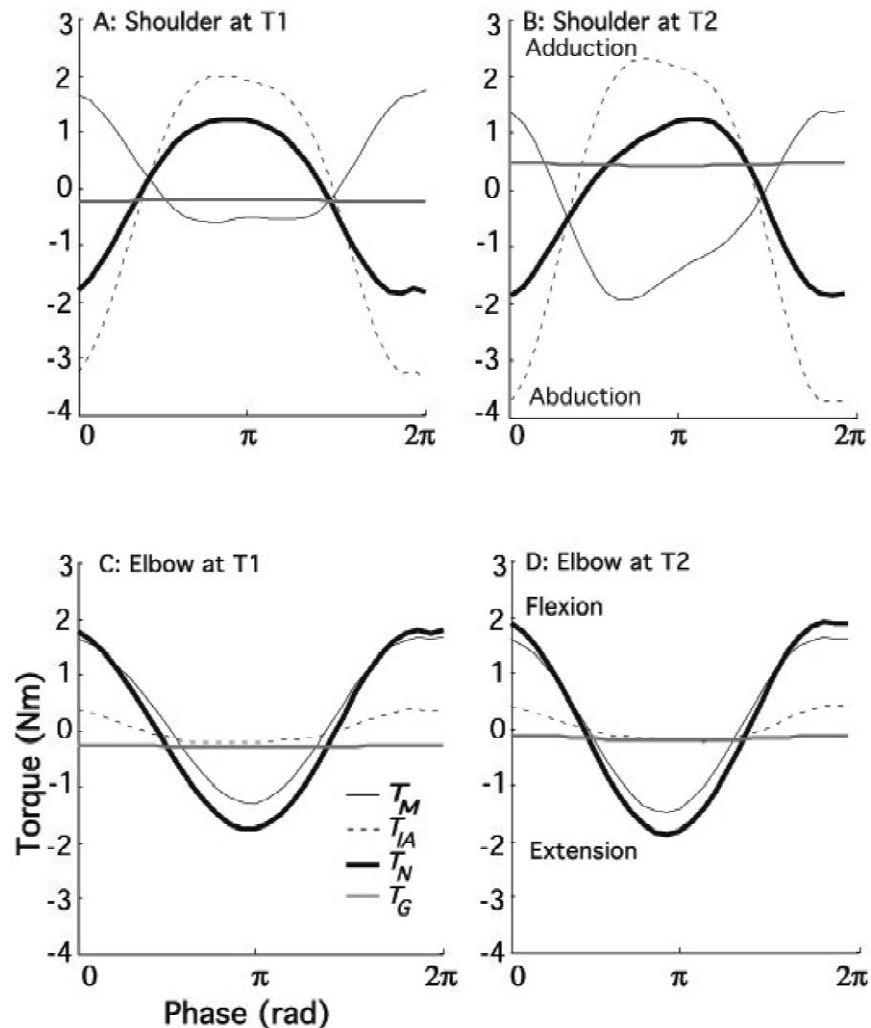


Fig. 10. Mean torque profiles during the steady state segment prior to the discrete transition. These profiles are representative for the second group of participants 2, 4, and 6. The notation is identical to Fig. 9.

3.2.2. Joint torques at onset and during the discrete movement

In order to assess the torque pattern prior to and during the discrete movement we examined the time series of torques. Fig. 11 exemplifies an abduction trial of participant 1 in the naive condition with a frequently preferred ϕ_{KIN} of 4.83 rad (see Fig. 7). Similar to the mean steady state pattern of the same participant shown in Fig. 9, it shows that during the pre-transition elbow oscillations the muscle torque is antiphase with the interaction torque and the net torque mirrors the muscle torque, indicating that it is primarily the muscle torque that generates the overt movement. At onset time, marked by the first vertical line at time zero, muscle and net torques are still opposing the discrete initiation, but are then continued in their pre-transition shape and facilitate the discrete initiation. In contrast, the interaction torque runs in the opposite direction during the first portion of the discrete movement. In the interval until peak velocity, marked by the second vertical line, the signs of all three torques have changed.

The interaction torque profile is only slightly perturbed during the discrete movement. This highlights that the elbow oscillation was continued and only a small phase shift occurred (Fig. 8). Note that the gravitational torque is slightly raised in the new target position. From inspection of this single trial two questions need to be answered: does interaction torque assist the initiation of the discrete movement? Does interaction torque get utilized during the acceleratory portion of the discrete translation?

To answer question 1 the values of each of the three shoulder torque components $T_{S,IA}$, $T_{S,M}$, $T_{S,N}$ at the moment of discrete movement initiation were evaluated as to whether or not they aided the initiation of the discrete shift. Table 3 summarizes the results of this analysis. In abduction trials, $T_{S,IA}$ act in the direction of the discrete shift in 40% and 46% of trials in blocks 1 and 2, respectively. This result does not support the hypothesis that interaction torques assist the translatory movement. Note also, that predictions for initiation phase derived from the exemplary mean torque patterns in Figs. 9A and 10A

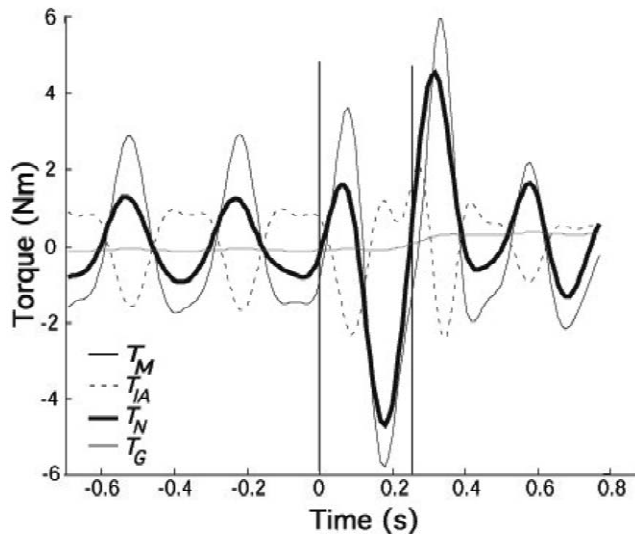


Fig. 11. Torques before and after the discrete transition in a single trial. The trial involved shoulder abduction in the naive condition. Negative torques accelerate the joint into the adduction direction. The first vertical line at time zero marks the time of the onset of the discrete movement t_{EMG} . The second vertical line marks the time of maximum velocity in the shoulder trajectory during the discrete transition. The phase of onset ϕ_{KIN} in this trial was 4.83 rad.

do not correspond to the preferred phase window between π and 2π rad found in the kinematic analysis above (Fig. 7). Examining $T_{S,M}$ and $T_{S,N}$ for abduction trials, the percentages for supporting muscle torques are close to chance. The results are slightly more favorable for adduction trials which show 61% and 63% of trials with positive $T_{S,IA}$ in the two blocks. Note that for a uniform distribution of onset phases $\sim 50\%$ of trials should show positive interaction torques in both abduction and adduction (Figs. 9B and 10B). Muscle torque more frequently resists the discrete transition with only 35% and 24% assisting the discrete shoulder adduction, consistent with uniformly distributed phase across trials. Finally, net torques also did not appear to be a criterion for the discrete initiation and the percentage values were close to 50%. In sum, the hypothesis that the discrete onset is timed to take advantage of interaction torques was not supported by the observed clustering of onset phases. For abduction trials this hypothesis was contradicted, for adduction trials, the

Table 3

Sign analysis of the three shoulder torques $T_{S,IA}$ (interaction torque), $T_{S,M}$ (muscle torque), and $T_{S,N}$ (net torque) at the moment of discrete movement onset (t_{EMG}). For each block and direction, the percentage of trials in which the respective torque component at the shoulder assisted the discrete movement is reported (%)

Torques	Block 1		Block 2	
	Abduction	Adduction	Abduction	Adduction
$T_{S,IA}$	40	61	46	63
$T_{S,M}$	50	35	59	24
$T_{S,N}$	49	56	58	47

data were equivalent. Muscle and net torques did not appear to be criteria for the timing of the discrete initiation and hence did not support hypothesis 2.

In a second step, we asked whether torques were utilized during the discrete movement. To this end, we analyzed the torques acting at the shoulder during the first segment of the discrete transition from t_{EMG} to the time of maximum discrete velocity (Fig. 11). If interaction torques were exploited, $T_{S,IA}$ should be predominantly positive in the accelerating segment of the adduction trials. For abduction trials, this sign prediction is reversed. To evaluate whether interaction torques assisted the discrete movement, the integral of $T_{S,IA}$ was computed across the accelerating segment. Subsequently, the results were dichotomized into trials where interaction torques were assisting and opposing the movement direction. For each block and direction the percentage of assisting trials was counted. In block 1, $T_{S,IA}$ assisted the acceleration of the discrete joint in 43% of trials in the adduction direction, and 40% of trials in the abduction direction. In block 2, $T_{S,IA}$ assisted the discrete movement in 45% of trials in adduction and only 28% of trials in abduction.

4. Discussion

The study examined a task that explicitly cut across the distinction into discrete and rhythmic movements, a dichotomy that is commonly adopted in research in motor control. The overarching goal of our present work is to reveal systematic phenomena that arise in such complex tasks where rhythmic and discrete elements have to be combined. Do joint trajectories, and consequently the endeffector trajectory, reflect (complex) features that are specific to the merging of (simpler) discrete and rhythmic elements?

Several previous studies have already investigated a similar single-joint task where, in contrast, both movement components were confined to a single-joint elbow rotation [1,7,54,56–58]. Following the same instructions, participants manifested systematic interactions between the two movement components. The central and robust result was that initiation of the discrete action was limited to a small window of the oscillatory cycle. This result was interpreted as a competition between the two signals for discrete and rhythmic movements. We replicated the major results in a model that posited a pattern generator for which the control signals were superimposed [7]. Following these experimental and modeling results, the first purpose of the present experiment was to test whether the observed constraints between rhythmic and discrete elements were generalizable to multi-joint intralimb coordination. Hypothesis 1 states that the coupling constraints between rhythmic and discrete elements are generic for the execution of two movement primitives in single- and multi-joint performance. If this hypothesis is supported, then the

mutual interactions are likely to reside not at the level of peripheral segmental dynamics but at some higher level of the central nervous system.

Extending analyses from single- to multi-joint movements needs to address a new central feature of multi-joint movements—the presence of intersegmental torques. Hence, the alternative hypothesis 2 states that the initiation of a voluntary discrete movement is determined by torque profiles generated by the ongoing rhythmic movement where intervals of movement assisting torques would be preferred for the initiation of discrete movements. This hypothesis extends from research that has proposed that the CNS has an internal model of the limb dynamics and skilled actions make use of such passive dynamical properties [10,11,25,42,43,45].

The chosen task raised one further issue: although the two-joint movements were confined to a planar surface, and thereby apparently non-redundant, the direction of the oscillatory amplitude was not prescribed. Therefore, the task was redundant during the steady state oscillatory segments where the ‘rubbing’ action could be performed with any combination of elbow and shoulder joint amplitudes. In contrast, the target-to-target translation had to be performed with a specific shoulder angle change. Hence, a third expectation was that in the self-selected condition, joint angle combinations would be preferred that facilitated the task to initiate a discrete movement as fast as possible. Specifically, the reaction time of the discrete action was expected to be shorter and the onset of the discrete movement would not be constrained in the naive performance.

4.1. Kinematic and EMG analysis

4.1.1. Steady state oscillation and its perturbation

A first focus of the data analyses was on the steady state oscillatory performance before and after the discrete movement. Given the instructional emphasis on maintaining the oscillation throughout the displacement, we scrutinized whether oscillation parameters before and after the transition remained identical. Neither amplitudes nor periods showed a marked change. The only result was that in the instructed condition the periods tended to become slightly faster after the termination of the initial pacing signal. This overall persistence in the oscillation converges with the previous findings in single-joint movements where only a small acceleration (10 ms) in the post-transition segment was observed. This change was probably due to the wider range of pacing periods, including ones that were much slower than the preferred one (1000 ms). Note that in this experiment the initial pacing period of 300 ms was close to the period preferred by the participants. This result is a necessary but not sufficient evidence for the assumption that the oscillation was continuously active even during the discrete movement and remained unchanged

throughout the entire trial. This assumption was an explicit component of the previous modeling [7,56].

Comparison of steady state parameters for both joints before and after the discrete movements also showed that joint recruitment did not differ between the two instructional conditions. Participants tended to use almost exclusively the distal joint for the rhythmic task, regardless of whether they received instructions to only move their elbow joint, or whether they simply intended to oscillate around a target in 2D. The observed coupling constraints could therefore not be attributed to the ‘artificial’ instruction-induced separation of the two movement components. Very small amplitude oscillations were also observed in the shoulder joint, but they were indistinguishably present in both blocks. Hence, it is likely that they served a stabilizing purpose. The nature of these movements is examined further in the torque analysis below.

This preference for isolated elbow rotations can be understood from a biomechanical perspective: movements that only involve the distal limb segment require less inertia to be overcome and are therefore more energetically efficient. Yet, such joint isolation produces curvilinear endpoint trajectories. This is different to what is observed in many studies on discrete reaching movements, where typically straight paths are selected which require the simultaneous involvement of two or more joints [9,12,15,37]. To ensure a direct path of the endpoint, both joint trajectories need to show common initiation and termination, and, depending on the target location, different angular velocities are required [5,6]. This contrast points to a potentially fundamental difference between discrete and rhythmic components: while rhythmic movements are back and forth movements around one axis of rotation, that is, their control is anchored in intrinsic or joint space coordinates, discrete movements displace the endeffector from one point in external space to another, that is, their recruitment is oriented in extrinsic space. This can be seen as another argument for the distinction into discrete and rhythmic control primitives. For an overview of theoretical approaches that propose movement planning in an intrinsic versus extrinsic reference frame see Ref. [61].

This invariance of the oscillatory parameters in the elbow movements was accompanied by the transient resetting of the oscillation phase due to the discrete shoulder movement. Regardless of the experimental condition, the cycle during or directly following the discrete movement was predominantly shortened by an average of 1.08 rad. This transient acceleration of the cycles was also indicated in the EMG signal. As Fig. 3 illustrates, the discrete bursts in the shoulder muscles were accompanied by high activity in the elbow muscles. The effect of resetting was robust and invariant across all conditions and independent of other factors such as the phase of the discrete initiation. With a view to possible control schemes for the integration of discrete and rhythmic elements it is

important to emphasize that such transient resetting of the oscillatory phase is a hallmark of nonlinear autonomous oscillators. Such perturbations of the oscillation therefore need not be interpreted as an explicit termination and initiation of the rhythm [60]. The conclusion from above that an oscillatory regime was continuously active during the discrete movement can therefore be sustained. The same prevailing phase advances were seen in the single-joint task. This observation provides support that the constraints between rhythmic and discrete elements is similar across tasks with different joint involvement and hence, reside at some higher level of the central nervous system (hypothesis 1).

While the kinematic traces showed relatively little shoulder involvement during the steady state segments—in some participants their shoulder joints were close to being stationary—the EMG measures of the posterior and anterior deltoid showed small but consistent rhythmic bursts. Notably, shoulder muscles were simultaneously active in an antiphasic relation to the triceps and brachioradialis bursts responsible for elbow flexion and extension. (Relative phase appeared to be slightly larger than π rad, but this is probably due to the shape of the EMG burst which can bias the determination of maximum activity within each cycle.) This pattern of activity indicated co-contraction in the shoulder which had most likely a stabilizing effect compensating for the interaction torques that were generated by the ongoing elbow activity. Such compensation of interaction torques in the stationary joint in single-joint reaching tasks was also demonstrated by Gribble and Ostry [19]. A fine-grained analysis of EMG activity and torque profiles in both single- and two-joint movements showed that the EMG bursts in stationary or adjacent joints slightly preceded the maxima in the respective interaction torques and the phasic EMG activity was scaled to the magnitude of these torques. For the task presently under scrutiny, this concurrent stabilizing activity in the shoulder muscles becomes the constraining factor when the additional discrete movement is initiated in the shoulder joint, as can be seen in the calculations of the onset of the discrete action.

4.1.2. *Timing and phasing of the discrete movement initiation*

The initiation of the discrete abduction movement when calculated as phase of ongoing EMG activity of the prime mover for the discrete abduction action occurred at a phase close when the burst would have happened without discrete movement, i.e. close to 2π rad. This result is in close replication of the single-joint results and in support of hypothesis 1: a discrete movement to be performed by an already rhythmically active synergy is limited to begin at the moment where a rhythmic burst would have occurred. In related work this finding is referred to as EMG burst synchronization or phase entrainment [53,54,56,57]. This initiation constraint was similar for both instructional

conditions and, counter to expectation, self-guided performance did not facilitate the initiation. Note that this rhythmic activity was not primarily generated for a voluntary rhythmic action of the shoulder, but rather it was compensatory activity countering intersegmental torques from the elbow.

Muscle activation for the initiation of different point-to-point planar movements involving two or three joints was examined extensively by Hasan and co-workers and Ghez and co-workers [13,16,27,30,31]. Analysis of a wide range of discrete movement extents, locations, and directions in the arm's workspace led to the conclusion that spatial direction of the endeffector point with respect to the initial forearm orientation and extent were important variables controlled by the motor system. Specifically, Karst and Hasan [27] showed that spatial direction proved to be the best predictor for the selection of the initiating muscle synergy. Relevant to the present study is that the discrete movements of the present experiment were characterized by direction angles of 153° (from T1 to T2) and 66° (from T2 to T1) (for details see Ref. [27]). For the T1→T2 movement, shoulder abduction was observed first and comparatively high activity could be expected in the posterior deltoid. Hence, increased activity in this muscle can be regarded as the best indicator for the initiation of the discrete shoulder movement. For the T2→T1 movement, shoulder adduction initiated the discrete movement and the shoulder adductor anterior deltoid could be expected to signal the movement initiation [27]. Note though, that this study measured the clavicular portion of the pectoralis major as the primary shoulder adductor.

Given the evidence of neural constraints for the abduction movement, it needs consideration why shoulder adduction did not yield the same pattern. One first possible reason for this lack of result is that the muscle chosen for measuring shoulder adduction was the anterior deltoid, which proved to be not ideal. The rhythmic activity was typically less pronounced and determination of the discrete onset was more difficult in this muscle. The pectoralis major might have been the better choice (see for a similar note Refs. [19,27]). Another difference between the two movement directions was the effect of gravity due to the inclined table. As further detailed below, gravitational torque tended to assist the movement in the adduction direction, while posing little resistance to the abduction direction. It was potentially this additional hurdle that may have influenced the consistency in the results. Thirdly, the two movement directions are not isotropic when the inertial resistance to different movement directions is considered [16,23,40,41]. Note that movement directions orthogonal to the forearm orientation present the least inertia for accelerating a movement from rest. Comparing the direction angles of the two discrete movements, the adduction movement deviated by 17° from a right angle, while the abduction movement deviated by 63° from a right angle. This may suggest that abduction was more

constrained to a ‘facilitatory phase window’ of the rhythmic activity due to the higher inertial resistance. However, this conclusion needs to be taken with caution as this analysis neglects the effects of acceleration- and velocity-dependent torques prevalent during the ongoing rhythmic movement. Future work will have to address the dependency of the initiation constraint on the location and direction of the discrete movement.

Reaction times did not show any variation as a function of the experimental conditions nor of the trigger phase. At first, this result seems at odds with the reported results of a modal distribution for ϕ_{EMG} and ϕ_{KIN} . However, there was a wide range of reaction times spanning from 50% (150 ms) to 170% (500 ms) of a cycle time (300 ms). Hence, the supra-threshold activity indicating movement onset may be delayed to occur one additional cycle after the trigger signal. This has the effect of making reaction time a variable quantity, while ϕ_{EMG} shows the systematic behavior. One result of this potential delay is that some reaction times were remarkably long compared to auditory premotor reaction times measured in typical single-task settings. However, the relatively long reaction times may also reflect interference or an inhibitory effect from the ongoing rhythmic activity. In general terms, longer reaction times in more complex tasks has been reported numerous times since the studies by Hick and Hyman and attributed to increased processing demands [22,26]. For the specific combination of discrete and rhythmic movements [7] reported longer reaction times for a more complex task variation.

The present findings are not consistent with the ones reported by Michaels and Bongers [36], Latash [33] and De Rugy and Sternad [7] who reported modulations of reaction time as a function of the oscillatory phase. On the other hand, the results of these two studies were also not identical and other studies also reported an absence of modulation [32]. De Rugy and Sternad [7] proposed an explanation for these inconsistent findings based on more technical issues about the onset detection as well as on theoretical arguments about the underlying mechanisms for reaction time modulation. One further explanation for the lack of effects is that the number of trials per condition was relatively small for a random variable to reveal systematic effects. Finally, it is of interest that the self-selected performance did not facilitate initiation of the discrete movement. However, this again comports with the lack of differences seen in the kinematic parameters between the naïve and controlled instructions.

4.1.3. Characteristics of the discrete movement

Was the discrete movement affected by the on-going oscillation? Although participants were asked to react and move their hand as fast as possible, the average peak velocity was only 177°/s. This is remarkably slow compared to rapid single-joint movements as reported in the literature. For instance, Gottlieb and co-workers report for

40° elbow joint movements peak velocities between 500 and 600°/s [17,18]. This comparison, however, has to take into account that in the present task the movement was performed by the shoulder joint and consequently must be expected to be slower due to its higher inertia. And yet, the difference is remarkably large and must be at least partially attributed to the fact that the discrete movement is started from within an ongoing oscillation. This interpretation is also supported by our previous finding in the single-joint task where peak velocities were also lower than the ones reported for point-to-point discrete movement in the same elbow joint [57,58]. For a similar task performed by two arms, Wei et al. [59] showed that even when the discrete movement was performed by the other arm, peak velocity was attenuated by the oscillation performed by the other arm and scaled with the oscillatory frequency. Note also, that peak velocity decreased with slower oscillation periods, supporting the influence exerted by the ongoing oscillation. Hence, the result is in general agreement with hypothesis 1. It is also important to point out that a slowing of the discrete movement is not a trivial result and, logically, the opposite result could have been hypothesized. Comparing rhythmic and discrete performance in a Fitts’ pointing task, Guiard [20,21] argued that cyclic performance is advantaged in a speed–accuracy task because the initial impulse of each back and forth movement is facilitated by the potential energy stored in the muscular tissues. Although Guiard did not report peak velocities, it can be extrapolated from this reasoning that peak velocities should be higher.

In sum, all kinematic results largely replicated what was reported for single-joint movements and thereby provide cumulative support for hypothesis 1. One major qualification though is that the initiation of shoulder adduction was not constrained. Yet, as in multi-joint movements inter-segmental dynamics becomes a major factor in the performance, the question remains open to what degree joint torques are responsible for the patterns observed. Is the preferred phase of initiation one where interaction torques aid in the direction of the discrete movement?

4.2. Kinetic analysis

A comparison between the systematically preferred phases of onset and the mean torque profiles in the abduction trials will provide an answer. For this comparison ϕ_{KIN} has to be considered, as this measure is referenced against the elbow joint angle (and not the EMG activity). If interaction torques were utilized, as predicted by hypothesis 2, then ϕ_{KIN} for discrete shoulder abduction should favor values between $3\pi/2$ and $\pi/2$ rad. For adduction trials ϕ_{KIN} should be between $\pi/2$ and $3\pi/2$ rad. Given the modal distribution around $3\pi/2$ rad, ranging between π and 2π rad, this expectation was only marginally supported. During half of the range of the preferred onset phases, the interaction torques worked

against the direction of the discrete abduction movement. For the adduction movements this comparison could not be made because systematic kinematic onset phases were missing. Conversely, if existent muscle torques were exploited, then the remaining segment of the cycle should be favored. Again, this argument could only partially be supported as the mode of the ϕ_{KIN} distribution around $3\pi/2$ rad was just at the boundary of the windows. Hence, no clear picture emerges from this comparison.

However, participants showed two different types of torque profiles. Therefore, analyses of individual trials were performed where the values of interaction and muscle torques at each onset were evaluated as assisting or resisting the movement direction. The proportion of trials where interaction torques or muscle torques assisted was close to 50% or chance, specifically in abduction trials. The count is slightly more favorable in adduction trials where interaction torques assist in $\sim 60\%$ of the trials, yet this is only a small bias. In adduction trials muscle torques more frequently resist the discrete transition with only 30% continuing their direction into the discrete initiation.

In a third step we calculated the integral of interaction torques across the interval between movement onset and the time of its peak acceleration. However, the binary summary of the analysis similarly documents that in none of the experimental conditions interaction torques were taken advantage of for the performance of the discrete transition. Concluding from these negative results, it must be muscle torque that overrode opposing motion-dependent passive torques producing the necessary joint acceleration in the discrete movement direction. Specifically, in abduction trials, where a predominant phase of initiation was identified, the onset was timed such that participants overrode the opposing mechanical torques. None of the analyses could identify differences between the naïve and the instructed conditions. These results contradict hypothesis 2. The discrepancy may be attributed to the fact that the presently examined task had reaction time demands, whereas the reports on utilization of mechanical aspects were found in self-guided movements and were typically found to improve with practice.

While the interaction between control signals for rhythmic and discrete primitives can be argued as support for hypothesis 1, it indirectly also can be seen as some support for hypothesis 2. It must be noted that the rhythmic activity in the shoulder muscles, which is the constraining factor for the discrete initiation, is most likely compensatory activity that stabilizes the shoulder joint in the face of torques acting from the moving elbow. Hence, passive torques generated by the elbow onto the shoulder joint create electromyographic activity that becomes significant for limiting the actions at the shoulder joint. In this sense, one might say that interaction torques do, in a secondary fashion, provide the constraints for joint actions.

In conclusion, results from the kinematic and kinetic analyses together were consistent with hypothesis 1,

suggesting that it is predominantly neural interactions that set constraints upon the combination of rhythmic and discrete movements. Analysis of torque profiles ruled out that utilization of interaction torques is the predominant criterion for the coupling of discrete with rhythmic movements (hypothesis 2). However, hypothesis 2 is not entirely contradicted as these torques from moving joints generate compensatory muscle activity in stationary joints that then presents constraints on the activation of movement in these joints.

5. Uncited reference

[48]

Acknowledgements

This research was supported by the National Science Foundation, SBR #97-1031297 and BCS-0096543.

References

- [1] S.V. Adamovich, M.F. Levin, A.G. Feldman, Merging different motor patterns: coordination between rhythmical and discrete single-joint movements, *Exp. Brain Res.* 99 (2) (1994) 325–337.
- [2] P.G. Amazeen, E.L. Amazeen, M.T. Turvey, Dynamics of human intersegmental coordination: theory and research, in: D.A. Rosenbaum, C.E. Collyer (Eds.), *Timing of Behavior: Neural, Computational, and Psychological Perspectives*, MIT Press, Cambridge, MA, 1998, pp. 237–259.
- [3] L.B. Bagesteiro, R.L. Sainburg, Handedness: dominant arm advantages in control of limb dynamics, *J. Neurophysiol.* 88 (5) (2002) 2408–2421.
- [4] J.J. Buchanan, J.A.S. Kelso, G.C. de Guzman, Self-organization of trajectory formation. I. Experimental evidence, *Biol. Cybern.* 76 (4) (1997) 257–274.
- [5] D. Bullock, S. Grossberg, Adaptive neural networks for control of movement trajectories invariant under speed and force rescaling, *Hum. Movement Sci.* 10 (1991) 3–53.
- [6] D. Bullock, S. Grossberg, The VITE model: a neural command circuit for generating arm and articulated trajectories, in: J.A.S. Kelso, A.J. Mandell, M.F. Shlesinger (Eds.), *Dynamic Patterns in Complex Systems*, World Scientific, Singapore, 1988, pp. 305–326.
- [7] A. De Rugy, D. Sternad, Interaction between discrete and rhythmic movements: reaction time and phase of discrete movement initiation against oscillatory movements. *Brain Res.*, in press.
- [9] M. Desmurget, M.I. Jordan, C. Prablanc, M. Jeannerod, Constrained and unconstrained movements involve different control strategies, *J. Neurophysiol.* 77 (1997) 1644–1650.
- [10] N.V. Dounskaia, S.P. Swinnen, C.B. Walter, A.J. Spaepen, S.M.P. Verschueren, Hierarchical control of different elbow–wrist coordination patterns, *Exp. Brain Res.* 121 (1998) 239–254.
- [11] N.V. Dounskaia, S.P. Swinnen, C.B. Walter, A principle of control of rapid multijoint movements, in: J.M. Winters, P.E. Crago (Eds.), *Biomechanics and Neural Control of Posture and Movement*, Springer, New York, 2000, pp. 390–404.
- [12] T. Flash, N. Hogan, The coordination of arm movements: an experimentally confirmed mathematical model, *J. Neurosci.* 5 (7) (1985) 1688–1703.

- [13] C. Ghez, J.W. Krakauer, R.L. Sainburg, M.F. Ghilardi, Spatial representation and internal models of limb dynamics in motor learning, in: M.S. Gazzaniga (Ed.), *The New Cognitive Neurosciences*, MIT Press, Cambridge, MA, 2000.
- [14] D. Goodman, J.A.S. Kelso, Exploring the functional significance of physiological tremor: a biospectric approach, *Exp. Brain Res.* 49 (1983) 419–431.
- [15] J. Gordon, M.F. Ghilardi, C. Ghez, Accuracy of planar reaching movements: I. Independence of direction and extent, *Exp. Brain Res.* 99 (1994) 97–111.
- [16] J. Gordon, M.F. Ghilardi, S.E. Cooper, C. Ghez, Accuracy of planar reaching movements. II. Systematic extent errors resulting from inertial anisotropy, *Exp. Brain Res.* 99 (1994) 112–130.
- [17] G.L. Gottlieb, Muscle activation patterns during two types of voluntary single-joint movements, *J. Neurophysiol.* 80 (4) (1998) 1860–1867.
- [18] G.L. Gottlieb, D.M. Corcos, G.C. Agarwal, Strategies for the control of voluntary movements with one mechanical degree of freedom, *Behav. Brain Sci.* 12 (1989) 189–250.
- [19] P.L. Gribble, D.J. Ostry, Compensation for interaction torques during single- and multi-joint movements, *J. Neurophysiol.* 82 (5) (1999) 2310–2326.
- [20] Y. Guiard, On Fitts' and Hooke's law: simple harmonic movements in upper-limb cyclical aiming, *Acta Psychol.* 82 (1993) 139–159.
- [21] Y. Guiard, Fitts' law in the discrete vs. cyclical paradigm, *Hum. Movement Sci.* 16 (1997) 97–131.
- [22] W.E. Hick, On the rate of gain of information, *Q. J. Exp. Psychol.* 4 (1952) 11–45.
- [23] N. Hogan, The mechanics of multi-joint posture and movement control, *Biol. Cybern.* 52 (1985) 315–331.
- [24] J.M. Hollerbach, T. Flash, Dynamic interactions between limb segments during planar arm movement, *Biol. Cybern.* 44 (1982) 67–77.
- [25] M.G. Hoy, R.F. Zernicke, The role of intersegmental dynamics during rapid limb oscillations, *J. Biomech.* 19 (10) (1986) 867–877.
- [26] R. Hyman, Stimulus information as a determinant of reaction time, *J. Exp. Psychol.* 45 (1953) 188–196.
- [27] G.M. Karst, Z. Hasan, Initiation rules for planar, two-joint arm movements: agonist selection for movements throughout the workspace, *J. Neurophysiol.* 66 (5) (1991) 1579–1593.
- [28] G.M. Karst, Z. Hasan, Timing and magnitude of electromyographic activity for two-joint arm movements in different directions, *J. Neurophysiol.* 66 (1991) 1594–1604.
- [29] J.A.S. Kelso, *Dynamic Patterns: The Self-organization of Brain and Behavior*, MIT Press, Cambridge, MA, 1995.
- [30] G.F. Koshland, Z. Hasan, Selection of muscles for initiation of planar, three-joint arm movements with different final orientations of the hand, *Exp. Brain Res.* 98 (1) (1994) 157–162.
- [31] J.W. Krakauer, Z.M. Pine, M.F. Ghilardi, C. Ghez, Learning of visuomotor transformations for vectorial planning of reaching trajectories, *J. Neurosci.* 20 (23) (2000) 8916–8924.
- [32] M. Lakie, N. Combes, There is no temporal relationship between the initiation of rapid reactive hand movements and the phase of enhanced physiological tremor in man, *J. Physiol.* 523 (2) (2000) 515–522.
- [33] M.L. Latash, Modulation of simple reaction time on the background of an oscillatory action: implications for synergy organization, *Exp. Brain Res.* 131 (2000) 85–100.
- [34] K. Matsuoka, Sustained oscillations generated by mutually inhibiting neurons with adaptations, *Biol. Cybern.* 52 (1985) 367–376.
- [35] K. Matsuoka, Mechanisms of frequency and pattern control in the neural rhythm generators, *Biol. Cybern.* 56 (1987) 345–353.
- [36] C.F. Michaels, R.M. Bongers, The dependence of discrete movements on rhythmic movements: simple RT during oscillatory tracking, *Hum. Movement Sci.* 13 (1994) 473–493.
- [37] P. Morasso, Spatial control of arm movements, *Exp. Brain Res.* 42 (1981) 223–227.
- [38] P. Morasso, V. Sanguineti, From cortical maps of the control of muscles, in: P. Morasso, V. Sanguineti (Eds.), *Self-organization, Computational Maps, and Motor Control*, Elsevier Science, Genova, Italy, 1997, pp. 547–591.
- [39] D.A. Rosenbaum, L.D. Loukopoulos, R.G.J. Meulenbroek, J. Vaughan, S.E. Engelbrecht, Planning reaches by evaluating stored postures, *Psychol. Rev.* 102 (1) (1995) 28–67.
- [40] P.N. Sabes, M.I. Jordan, Obstacle avoidance and a perturbation sensitivity model for motor planning, *J. Neurosci.* 17 (1997) 7119–7128.
- [41] P.N. Sabes, M.I. Jordan, D.M. Wolpert, The role of inertial sensitivity in motor planning, *J. Neurosci.* 18 (1998) 5948–5957.
- [42] R.L. Sainburg, D. Kalakanis, Differences in control of limb dynamics during dominant and nondominant arm reaching, *J. Neurophysiol.* 83 (2000) 2661–2675.
- [43] R.L. Sainburg, C. Ghez, D. Kalakanis, Intersegmental dynamics are controlled by sequential anticipatory, error correction, and postural mechanisms, *J. Neurophysiol.* 81 (1999) 1045–1056.
- [44] S. Schaal, D. Sternad, R. Osu, M. Kawato, Rhythmic arm movement is not discrete, *Nat. Neurosci.*, in press.
- [45] K. Schneider, R.F. Zernicke, R.A. Schmidt, T.J. Hart, Intersegmental dynamics during the learning of a rapid arm movement, *J. Biomech.* 20 (1987) 816.
- [46] K. Schneider, R.F. Zernicke, R.A. Schmidt, T.J. Hart, Changes in limb dynamics during the practice of rapid arm movements, *J. Biomech.* 22 (8–9) (1989) 805–817.
- [47] K. Schneider, R.F. Zernicke, B.D. Ulrich, J.L. Jensen, E. Thelen, Understanding movement control in infants through the analysis of limb intersegmental dynamics, *J. Motor Behav.* 22 (4) (1990) 493–520.
- [48] B.C.M. Smits-Engelsman, G.P. Van Galen, J. Duysens, The breakdown of Fitts' law in rapid, reciprocal aiming movements, *Exp. Brain Res.* 145 (2002) 222–230.
- [49] J.F. Soechting, C.A. Terzuolo, An algorithm for the generation of curvilinear wrist motion in an arbitrary plane in three-dimensional space, *Neuroscience* 19 (4) (1986) 1393–1405.
- [50] G. Staude, Precise onset detection of human motor responses using whitening filter and the log-likelihood-ratio test, *IEEE Trans. Biomed. Eng.* 48 (11) (2001) 1292–1305.
- [51] G. Staude, W. Wolf, Objective motor response onset detection in surface myoelectric signals, *Med. Eng. Phys.* 21 (1999) 449–467.
- [52] G. Staude, R. Dengler, W. Wolf, The discontinuous nature of motor execution. I. A model concept for single-muscle multiple-task coordination, *Biol. Cybern.* 82 (1) (2001) 23–33.
- [53] G. Staude, R. Dengler, W. Wolf, The discontinuous nature of motor execution. II. Merging discrete and rhythmic movements in a single-joint system—the phase entrainment effect, *Biol. Cybern.* 86 (6) (2002) 427–443.
- [54] D. Sternad, Debates in dynamics: a dynamic systems' perspective to action and perception, *Hum. Movement Sci.* 19 (2000) 407–423.
- [55] D. Sternad, W.J. Dean, S. Schaal, Interaction of rhythmic and discrete pattern generators in single-joint movements, *Hum. Movement Sci.* 19 (2000) 627–665.
- [56] D. Sternad, A. de Rugy, T. Pataky, W.J. Dean, Interactions of discrete and rhythmic movements over a wide range of periods, *Exp. Brain Res.* 147 (2002) 162–174.
- [57] K. Wei, Discrete and rhythmic elements in uni- and bimanual tasks, Masters Thesis at the Pennsylvania State University.
- [58] K. Wei, G. Wertman, D. Sternad, Discrete and rhythmic components in bimanual actions, *Motor Control* 7 (2) (2003b) 134–155.
- [59] A.T. Winfree, *The Geometry of Biological Time*, Springer Verlag, New York, 1990.
- [60] D.M. Wolpert, Computational approaches to motor control, *Trends Cogn. Sci.* 1 (1997) 209–216.
- [61] V. Zatsiorsky, *Kinetics of Human Movement*, Human Kinetics, Champaign, IL, 2001.